OPTICAL SPECTROSCOPY OF GLASSES

PHYSIC AND CHEMISTRY OF MATERIALS
WITH LOW-DIMENSIONAL STRUCTURES

Series C: Molecular Structures

GENERAL EDITOR: E. MOOSER

OPTICAL SPECTROSCOPY OF GLASSES

Edited by

I. ZSCHOKKE

University of Basel Institute of Physics,
Department of Condensed Matter Physics

D. REIDEL PUBLISHING COMPANY

A MEMBER OF THE KLUWER  ACADEMIC PUBLISHERS GROUP

DORDRECHT / BOSTON / LANCASTER / TOKYO

Library of Congress Cataloging in Publication Data

CIP

Optical spectroscopy of glasses.

(Physics and chemistry of materials with low-dimensional structures. Series C, Molecular structures)
Includes index.
1. Glass—Spectra. 2. Glass—Optical properties.
I. Zschokke, I., 1933— II. Series.
QC464.G55068 1986 530.4'1 86—17712
ISBN-13: 978-94-010-8566-3 **e-ISBN-13: 978-94-009-4650-7**
DOI: 10.1007/978-94-009-4650-7

Published by D. Reidel Publishing Company.
P.O. Box 17, 3300 AA Dordrecht, Holland.

Sold and distributed in the U.S.A. and Canada
by Kluwer Academic Publishers,
101 Philip Drive, Assinippi Park, Norwell, MA 02061, U.S.A.

In all other countries, sold and distributed
by Kluwer Academic Publishers Group,
P.O. Box 322, 3300 AH Dordrecht, Holland.

EDITORIAL PREFACE

During the last fifteen years the field of the investigation of glasses has experienced a period of extremely rapid growth, both in the development of new theoretical approaches and in the application of new experimental techniques. After these years of intensive experimental and theoretical work our understanding of the structure of glasses and their intrinsic properties has greatly improved. In glasses we are confronted with the full complexity of a disordered medium. The glassy state is characterised not only by the absence of any long-range order; in addition, a glass is in a non-equilibrium state and relaxation processes occur on widely different time scales even at low temperatures. Therefore it is not surprising that these complex and novel physical properties have provided a strong stimulus for work on glasses and amorphous systems.

The strikingly different properties of glasses and of crystalline solids, e.g. the low-temperature behaviour of the heat capacity and the thermal conductivity, are based on characteristic degrees of freedom described by the so-called two-level systems. The random potential of an amorphous solid can be represented by an ensemble of asymmetric double minimum potentials. This ensemble gives rise to a new class of low-lying excitations unique to glasses. These low-energy modes arise from tunneling through a potential barrier of an atom or molecule between the two minima of a double-well. Although the microscopic nature of this two-state tunneling system is not yet clear, this concept has proven to be a very promising one for a better understanding of the fundamental processes and many anomalous properties. For experimental investigations advanced high-resolution laser techniques have proven to be a very powerful tool for studying these new characteristical phenomena.

The purpose of this volume is to provide a review of the current knowledge that has resulted from the great activity in the experimental and theoretical investigation of the static and dynamic spectroscopic properties of transparent glasses. We tried to find a balance between theoretical and experimental contributions. The majority of the articles are concerned with the shape and linewidth of optical transitions of guest impurities in a glass. The correlation between the coupling of a guest to the ensemble of two level systems of the host medium and the temperature and time dependence of the observed homogeneous optical linewidth of the guest, is currently a central question. Besides the scientific interest, the understanding of the general properties of optically active glasses has immediate technical consequences e.g. for laser technology, ceramics etc. To impart a feeling on this area, one of the contributions gives a state-of-the-art review of recent advances on the spectroscopic properties of a great variety of insulating inorganic glasses.

In the final article of the book the role of disorder, including fractal concepts, and the influence of random walks on the dynamics and the relaxation phenomena in an

amorphous system are analysed. This difficult problem is closely related to the transport properties in glassy materials, and therefore is of fundamental importance.

In a book like this, the scope is necessarily limited. Much of the extensive work which provided the foundations of this field and the names of the numerous scientists who have made key contributions to the development of our present understanding and the material presented in this book, are only found in the extensive lists of references. This book is intended to be of immediate interest to material scientists, physicists, chemists and scientists concerned with modern problems of condensed matter physics.

I wish to express my sincere gratitude to the authors for the careful preparation of their manuscript and their valuable collaboration in assembling this book.

Basel, July 1986 MRS I. ZSCHOKKE-GRÄNACHER

TABLE OF CONTENTS

DYNAMICAL THEORY OF OPTICAL LINEWIDTHS IN GLASSES

S. K. LYO
Sandia National Laboratories, Albuquerque, N.M. 87185, U.S.A.

1. Introduction

Many physical properties of amorphous solids are strikingly different from those of crystalline solids at low temperatures [1]. One of these anomalous properties, which is the subject of this chapter, is the low-temperature homogeneous optical linewidth of an optically active ion imbedded in a glass matrix. Recently there has been a considerable amount of experimental work [2—10] in this area due to advances in high-resolution spectroscopic techniques. The linewidths have been determined by fluorescence line-narrowing in inorganic glasses [2, 3] and by photochemical [5—9] and non-photochemical [10] hole-burning in organic glasses.

The linewidths are typically of the order of 30—500 MHz at 1 K and are orders of magnitude larger than those found in the crystalline solids at low temperatures. In some organic glasses, holewidths as large as a few cm^{-1} (10—100 GHz) were measured at 2 K [10b]. In amorphous materials the linewidth follows an unusual power-law temperature (T) dependence:

$$\hbar\Delta\omega \propto T^m \tag{1}$$

with the exponents in the range $1 \leqq m \leqq 2.2$ for various combinations of ions and amorphous hosts. The typical exponents observed so far are $m = 1$ [4, 7b, 10], $m = 1.33$ [7a], $m = 1.5$ [8], and $m \approx 2.0$ [2, 3, 6] at low temperatures (roughly below 20 K). In inorganic glasses [2, 3], the same power-law (i.e. $m \approx 2.0$) extends to room temperature. This behavior is in clear contrast with the standard T^7 dependence arising from two-phonon Raman processes at low temperatures or the activated exponential temperature dependence arising from Orbach processes in ordered solids [11]. The quadratic temperature dependence observed in inorganic glasses can be explained by a two-phonon Raman mechanism at high temperatures [2]. More detailed descriptions of the data are given in other chapters of this book.

After years of theoretical attempts to explain the anomaly [10, 12—21], it seems to be clear that the explanation is not attributable to conventional excitations known in crystalline solids alone. Naturally, we look into the possible role of the new class of low-energy excitations unique to glasses, namely, the so-called two-level systems (here designated as TLS in both singular and plural) which are known to give rise to other anomalies [1]. The low-energy modes arise from tunneling of an atom or a group of atoms between two energy minima of an asymmetric double-well through a potential barrier. A distribution of the energy asymmetry of the well depths and of the barrier heights gives a broad distribution

I. Zschokke (ed.), Optical Spectroscopy of Glasses, 1—21.

of energies and a nearly constant density of states for TLS [22, 23]. Although the original TLS model was proposed for explaining very low temperature phenomena (e.g. below 1 K) [22, 23], we are extending it to higher temperatures. The advantage of using TLS rather than phonons for interactions with optical ions lies in the fact that the ion-TLS coupling as well as the density of states of TLS does not decrease with decreasing temperature as rapidly as those of phonons. While phonons are not coupled directly to optical ions in our model, they play an important role in inducing tunneling-transitions in TLS.

The homogeneous linewidths are much smaller than the background inhomogeneous linewidths, which are of the order of a few hundred cm^{-1} in glasses [7, 24]. We will be concerned with the dynamical broadening of a line out of the quasi-uniform background (i.e. away from the wings), arising from modulations of the optical levels by TLS. The present treatment is based on earlier work by the author [16] for the short-time behavior of the spectral function and on recent work [25] for the long-time behavior. Emphasis is given to a simple picture for the line-broadening mechanism.

We begin with a brief description of the model Hamiltonian by defining the optical levels of an ion, the TLS Hamiltonian, ion—TLS interaction, and TLS—phonon coupling. This is followed by studies of two types of basic TLS—line modulation (i.e. dephasing) mechanisms using analogies with nuclear spin relaxation and second-order perturbation theory. These results are then used to describe the short-time and the long-time behaviors of homogeneous linewidths. This simple approach is then justified by a full Green's function theory. The paper is concluded with a brief summary.

2. Model Hamiltonian

The optical line at the energy $\hbar\omega_0$ is chosen by a laser line and corresponds to optical transitions between the ground ($n = 0$) and excited ($n = 1$) levels of impurity ions. The optical excitation energy $\varepsilon_{01} = \varepsilon_1 - \varepsilon_0$ (Figure 1) is much larger than other energy parameters such as the Debye acoustic phonon energy and the energy (E) of TLS. In a crystalline solid, the energy ε_{01} is modulated by lattice vibrations which cause phase interruptions and thereby linewidths. However, this contribution is too small to explain the linewidths in glasses as mentioned in Section 1. Therefore, we propose an impurity dephasing mechanism by TLS in glasses.

The basic idea is that a TLS atom or a group of atoms makes a rapid phonon-assisted tunneling motion between two local wells as illustrated in Figure 1. As a result, its coupling to the optical level n (= 0, 1) undulates by a small amount C_n, yielding a net modulation of $C_1 - C_0$ of the resonant optical transition energy. This mechanism is displayed in Figure 1 by solid lines connecting the optical levels and the atom in the wells. The motion associated with a TLS may also be rotational. The coupling between the ion and TLS is achieved by electric multipolar or phonon-exchange interactions [13, 16, 21, 26].

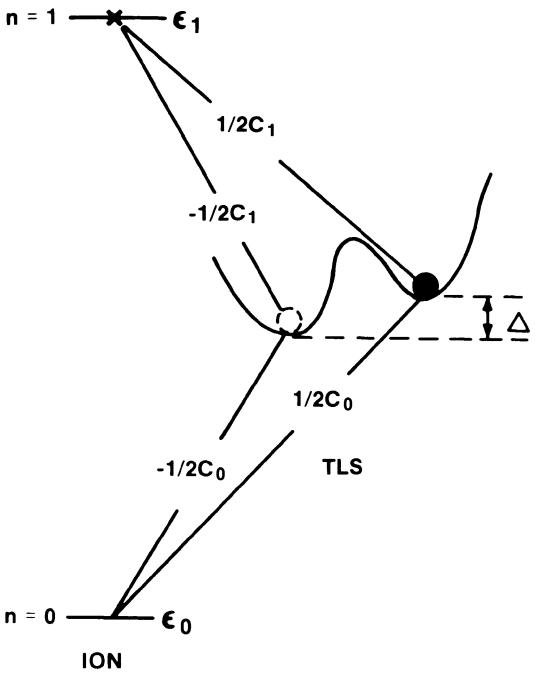

Fig. 1. Interaction of the ground ($n = 0$) and excited ($n = 1$) levels of an ion with an atom in TLS shown by an asymmetric double-well.

The dynamical part of the coupling of TLS to the nth level of the ion is then written conveniently by a 2×2 matrix [14, 16]:

$$\frac{1}{2} C_n \begin{bmatrix} 1 & 0 \\ 0 & -1 \end{bmatrix}_{\text{well}}, \tag{2}$$

where C_n is the difference of the coupling strengths at the two wells. The subscript 'well' means that we are in a local site representation; the wave function (ϕ_L) in the left well is orthogonal to that (ϕ_R) in the right well. The diagonal elements represent the coupling strengths at the right well (+1) and left well (−1) apart from a constant static part. The off-diagonal elements are proportional to the overlap of the wave functions and are ignored.

For TLS we use the Hamiltonian [22, 23]

$$\frac{1}{2} \begin{bmatrix} \Delta & t' \\ t' & -\Delta \end{bmatrix}_{\text{well}}, \tag{3}$$

again given in the site representation. Here Δ and $t'/2$ are the energy asymmetry of the wells and the tunneling integral, respectively. The energy needed for

hopping between the wells is provided by the deformation potential [22]

$$\frac{1}{2} B\varepsilon \begin{bmatrix} 1 & 0 \\ 0 & -1 \end{bmatrix}_{\text{well}}, \tag{4}$$

where ε is the strain and B the difference in the deformation potential constants for the two unperturbed wells.

The TLS Hamiltonian in (3) is diagonalized by the eigenfunctions $\Phi_{\pm}$ related to the site representation wave functions $\phi_{R,L}$ by

$$\Phi_s = t'[2E(E - s\Delta)]^{-1/2}\phi_R - s\left(\frac{E - s\Delta}{2E}\right)^{1/2}\phi_L, \quad (s = \pm 1), \tag{5}$$

with the eigenvalues $\frac{1}{2}sE$ and $E = [\Delta^2 + t'^2]^{1/2}$. The quantities in (2) and (4) can be transformed into the new diagonal representation by (5). The total Hamiltonian then reads in the new diagonal $\Phi_{\pm}$-representation [16]:

$$H = \sum_n \varepsilon_n \psi_n^\dagger \psi_n + \frac{1}{2} E\sigma^z + \frac{1}{2}\sum_n \psi_n^\dagger \psi_n \sum_\alpha V_n^\alpha \sigma^\alpha + \\ + \sum_q \left(n_q + \frac{1}{2}\right)\hbar\omega_q + \frac{1}{2}\sum_\alpha f^\alpha \varepsilon \sigma^\alpha. \tag{6}$$

In (6), $\psi_n^\dagger(\psi_n)$ is a Fermion creation (destruction) operator and $\psi_n^\dagger\psi_n = P_n$ $(= 0, 1)$ is the probability for the occupation of the optical level n. A pseudo spin-$\frac{1}{2}$ representation is used for TLS, which will be referred to as 'spin' at times hereafter. The quantity $\boldsymbol{\sigma}$ denotes the Pauli spin matrices with $\sigma^{\pm} = \sigma^x \pm i\sigma^y$. The superscript α is summed over $\alpha = z, +$, and $-$. The first three terms in (6) then represent an unperturbed optical ion, a single spin (TLS) with energy E, and interaction between them, respectively. The fourth term describes the phonon bath, with ω_q and n_q standing for the angular frequency and the occupation number of phonons with crystal momentum q. Finally, the last term in (6) represents the TLS—phonon coupling. The strain ε is assumed to be small. The spin—ion and spin—phonon coupling constants V and f are given by

$$V_n^z = \frac{C_n\Delta}{E}, \qquad V_n^{\pm} = \frac{\frac{1}{2}C_n t'}{E} \tag{7}$$

and

$$f^z = \frac{B\Delta}{E}, \qquad f^{\pm} = \frac{\frac{1}{2}Bt'}{E}. \tag{8}$$

Although a single spin is shown in (6) for simplicity, summation over all spins is implicitly assumed. The model Hamiltonian (6) forms the basis of our analysis.

The TLS of interest are those for which the energy barrier is sufficiently large (i.e. $t' < \Delta$) so that resonant tunneling between the two wells does not occur. For

these TLS (i.e. $t' < \Delta$) the correction to the eigenvalues due to tunneling is negligible so that the density of states of TLS is determined essentially by the distribution of Δ [22]. It is seen from (7) that the diagonal coupling is always larger than the off-diagonal coupling (i.e. $V_n^z > 2V_n^{\pm}$). Furthermore, for a small t' and a large Δ, the diagonal coupling is large and the off-diagonal coupling is small. This is easily understood from the fact that a large energy asymmetry, Δ, spatially separates the two eigenfunctions into the unperturbed wells (i.e. $\Phi_{\pm} \sim \phi_{\pm}$ in (5)), thereby enhancing the amount of the modulation of the coupling energy during phonon-assisted transitions.

3. TLS Line-Broadening Mechanism

The line-broadening mechanism is different for diagonal (V^z) and off-diagonal ($V^{\pm}$) spin—ion couplings. Although one can affect the other in a certain parameter regime through renormalization of the optical and TLS structures and by an interference effect, we attempt to contrast the differences by first considering modulation by the diagonal coupling in the absence of the off-diagonal coupling and vice versa for conceptual clarity. Fortunately this kind of description seems to be relevant to a wide class of systems at low temperatures. A discussion of the full combined effect of the diagonal and off-diagonal couplings will be postponed to Section 5.4.

3.1. DIAGONAL MODULATION

The diagonal part of spin—ion coupling (i.e. the third term of (6)) reads:

$$\frac{1}{2}\sum_n P_n V_n^z \sigma^z. \tag{9}$$

As a result of this coupling, the resonant optical transition will be shifted to $\varepsilon_{01} - \frac{1}{2}V^z$ and $\varepsilon_{01} + \frac{1}{2}V^z$ when the TLS is in the spin-down (i.e. $\sigma^z = -1$) state and spin-up (i.e. $\sigma^z = +1$) state, respectively. Here V^z is defined by $V^z = V_1^z - V_0^z$. As the atom rattles between the two wells, the resonant optical energy of the ion switches back and forth by an amount $\pm V^z$. The problem is then similar to the relaxation of a nuclear spin (corresponding to the ion) coupled to fluctuating electron spin σ^z, yielding a linewidth [17, 27]

$$\hbar\Delta\omega' = \hbar^{-1}\left(\frac{V^z}{2}\right)^2 \mathrm{Re}\int_0^{\infty} \langle \sigma^z(t)\sigma^z(0) - \langle\sigma^z\rangle^2\rangle \, \mathrm{e}^{-i\omega t}\,\mathrm{d}t$$

$$= \frac{(V^z)^2}{4\hbar}\,\mathrm{sech}^2\left(\frac{\beta E}{2}\right)\frac{\tau}{1+(\omega\tau)^2}. \tag{10}$$

Here Re means the real part, τ is the spin-lattice relaxation time of TLS,

$\beta = (k_B T)^{-1}$, and k_B is Boltzmann's constant. The quantity τ is a random parameter determined by the spin energy E and the tunneling integral t'. The 'nuclear spin' energy equals the optical shift $\hbar\omega = \frac{1}{2}V^z$, yielding

$$\hbar\Delta\omega' = (V^z)^2 \operatorname{sech}^2\left(\frac{\beta E}{2}\right) \frac{\hbar\tau}{4\hbar^2 + (\tau V^z)^2}. \tag{11}$$

When the damping of the TLS ($\hbar\tau^{-1}$) is much larger than V^z, namely, the spectral shift, the expression in (11) reduces to [2a, 16]

$$\hbar\Delta\omega_a' = (\tfrac{1}{2}V^z)^2 \hbar^{-1} \operatorname{sech}^2\left(\frac{\beta E}{2}\right) \tau. \tag{12a}$$

According to this result, the line becomes narrower for a faster phonon-assisted tunneling between the wells (i.e. for a smaller τ). This result of fast modulation is similar to motional narrowing in the spin relaxation problem.

On the other hand, if the damping of the TLS is much smaller than the spectral shift, we find from (11) [16]

$$\hbar\Delta\omega_b' = \operatorname{sech}^2\left(\frac{\beta E}{2}\right) \hbar\tau^{-1}. \tag{12b}$$

Therefore, in the slow modulation regime, the line broadens as the modulation rate (τ^{-1}) becomes faster (e.g. with increasing temperature). Also, the linewidth in (12b) is independent of the ion—TLS coupling strength! Of course, this does not mean that a spin at an infinite distance away from the ion gives a finite contribution to the linewidth. It means, however, that as long as the spin—ion coupling strength V^z is larger than the damping of the spin, it yields the linewidth in (12b) independent of the coupling strength (i.e. ion—spin distance). While a full microscopic proof of this claim with be given for an arbitrarily large V^z later in Section 5, this interesting result deserves an immediate and simple explanation, which is given below.

In order to understand how the linewidth is independent of ion—spin coupling strength for a large coupling, we consider second-order perturbation processes (Figure 2). The circled numbers there represent the order in the perturbation chain. In Figure 2(a) the ion makes a virtual interaction of strength $\frac{1}{2}V^z$ with the spin in the upper level in step 1. In step 2 the spin flips (by the last term in (6): $\frac{1}{2}f^-\varepsilon\sigma^-$) to the lower level by emitting a phonon q. In Figure 2(b) the steps 1 and 2 are reversed. The t-matrices for these processes are given by

$$t_{a,b} = \frac{\frac{1}{2}V^z}{\frac{1}{2}V^z} f^+ \langle n_q + 1 \,|\, \varepsilon \,|\, n_q \rangle, \tag{13}$$

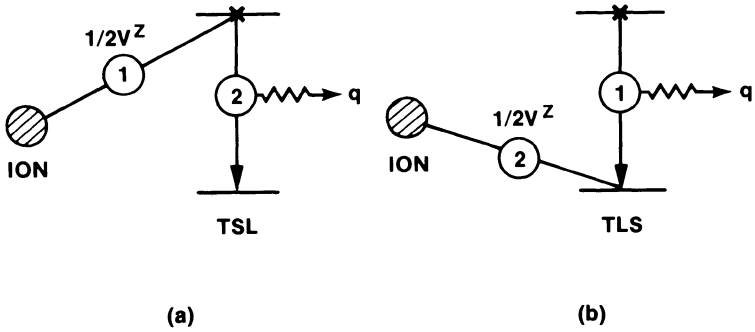

Fig. 2. Two-step processes for diagonal modulation. Directed wiggly lines and circled numbers indicate phonon-emission and the sequence in the perturbation chain, respectively.

where the quantity in the denominator denotes the intermediate energy which includes the optical shift. It is immediately seen from (13) that the quantity V^z cancels out. There are two more processes similar to those in Figure 2, but with the spin initially in the lower level. In these processes one phonon is absorbed to conserve the energy. The dephasing rate from these processes yields $\Delta\omega'_b$; using

$$\Gamma^{\pm} = 2\pi \sum_q (f^+)^2 \,|\langle n_q \pm 1 \,|\, \varepsilon \,|\, n_q\rangle|^2 \,\delta(E - \hbar\omega_q). \tag{14}$$

and

$$\hbar\tau^{-1} = \Gamma^- + \Gamma^+ = \Gamma^-[1 + e^{\beta E}], \tag{15}$$

we obtain the relationship in (12b). The quantities $\Gamma^{\pm}$ indicate the linewidths of the upper (+) and the lower (−) spin levels. The second equality in (15) is due to detailed balance.

3.2. Off-diagonal modulation

The contribution to the linewidth by the off-diagonal coupling $V_n^{\pm}$ (i.e. the third term of (6)) is evaluated in a similar way by employing the two-step processes [14] illustrated in Figure 3 for the case where the spin is initially in the upper level. In Figure 3(a) a virtual phonon of momentum q is emitted in step 1 (by the last term in (6): $\frac{1}{2}f^z\varepsilon\sigma^z$) and then the spin is flipped to the lower level by the ion—spin interaction $V_n^{\pm}$ in step 2. In Figure 3(b) the steps 1 and 2 are reversed so that one phonon is emitted in the lower level. The t-matrices for these processes are given by

$$t'_a = t'_b = \frac{V_n^-}{2E} f^z \langle n_q + 1 \,|\, \varepsilon \,|\, n_q\rangle. \tag{16}$$

The quantity E in the denominator represents the intermediate energy. Again, there are two more one-phonon-absorption processes similar to those in Figure 3

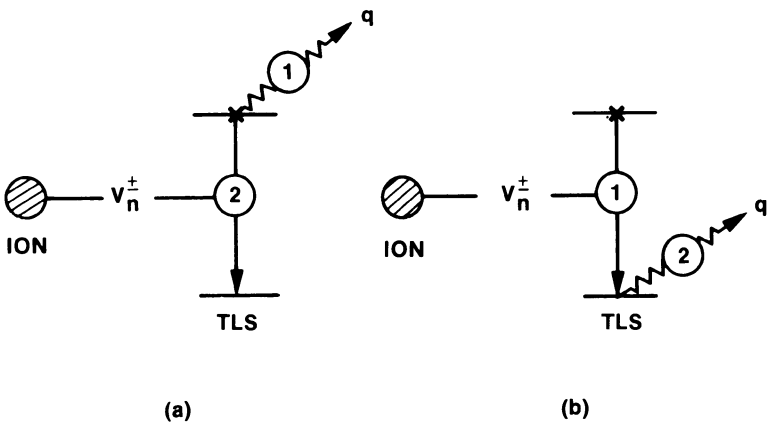

Fig. 3. Two-step processes for off-diagonal modulation. Directed wiggly lines and circled numbers indicate phonon-emission and the sequence in the perturbation chain, respectively.

but with the spin initially in the lower level. Combining these processes, and using (7), (8), (14), and (15), we find

$$\hbar\,\Delta\omega'' = \frac{1}{2}\,\hbar\tau^{-1}\sum_n \left(\frac{V_n^z}{E}\right)^2 \operatorname{sech}^2\left(\frac{\beta E}{2}\right). \tag{17}$$

This result is qualitatively different from that of diagonal modulation (i.e. Equation (11)) in that (1) the line always broadens with increasing rate (τ^{-1}) of modulation and that (2) only strongly coupled TLS adjacent to the ion make dominant contributions to $\Delta\omega''$ because of the strong quadratic dependence on V_n^z.

The result in (17) was originally proposed by Lyo and Orbach [14] (and studied in more detail by later authors [15, 20]) to explain the T^2-dependence of the linewidth data [2] of inorganic glasses in a wide temperature range $7 < T < 300$ K. The quadratic temperature dependence is obtained from (17) by using $\tau^{-1} \propto E^3$ (see (28)) and summing over E for a constant density of states of TLS. When the thermal energy $k_B T$ is much larger than the maximum TLS energy, a linear temperature dependence is obtained [14]. However, at low temperatures relevant to most of the recent data of organic glasses measured by hole-burning below 20 K down to 1 K or below, the above quadratic temperature will be modified. This follows from the fact that at low temperatures the coupling energy V_n^z in (17) is not small compared to the thermal TLS energy E. The latter should then be replaced by the renormalized energy

$$E_n = [(E + V_n^z)^2 + 4(V_n^+)^2]^{1/2}, \tag{18}$$

which is obtained from the first three terms in (6). Also, note that $\Delta\omega''$ is smaller than $\Delta\omega_b'$ in (12b). Since the damping $\hbar\tau^{-1}$ ($\propto E^3 \sim T^3$) becomes very small at low temperatures, the expression in (12b) is valid even for weakly coupled

TLS with $V^z \sim \hbar\tau^{-1}$. In this regime, $\Delta\omega''$ is smaller than $\Delta\omega_b'$ by a factor $\sim(V_n^z/E)^2 \ll 1$ and will not be considered until Section 5.3.

4. Homogeneous Linewidth

4.1. Spectral function

The lineshape is obtained by Fourier-transform of the spectral function:

$$F(t) = \exp\left(-i\omega_0 t - \frac{t}{2}\sum_{\text{TLS}}{}' \Delta\omega_i'\right), \tag{19}$$

where $\Delta w_i'$ is the dephasing rate given by (11) and the subscript i denotes TLS. The quantity ω_0 represents the frequency of the probe laser line. A microscopic study of the spectral function $F(t)$ will be presented later in Section 5.

The laser line excites the optical ions with perturbed energies resonant with $\hbar\omega_0$ out of the broad inhomogeneous background. The quantity $F(t)$ represents the spectral function of ions in the packet $\hbar\omega_0$. The perturbed energy of the ion equals the unperturbed resonance energy ε_{01} plus the sum of the spectral shifts $\frac{1}{2}V^z\sigma^z$ (cf. (9)) from all TLS interacting with it. A spin-flip from $\sigma^z = -1$ $(+1)$ to $\sigma^z = +1$ (-1) will cause a spectral shift, $+V^z$ $(-V^z)$. Therefore as a spin flips up (down), a line will be pulled up (down) out of the packet. Namely, only a down (up)-spin can pull up (down) a line, and these two processes should be weighted properly by Boltzmann factors. The quantity $\Delta\omega'$ in (19) contains this effect.

The quantity of interest is

$$\Phi(t) = \langle F(t)\rangle. \tag{20}$$

Here the angular brackets denote the configuration average and the average over the random TLS parameters. By carrying out the average [28], we find

$$\Phi(t) = \exp[-\tfrac{2}{3}\pi n\psi(t) - i\omega_0 t], \tag{21}$$

where n is the density of TLS and

$$\psi(t) = 6\int_0^\infty r^2(1 - \langle e^{-t\Delta\omega'/2}\rangle)\,dr. \tag{22}$$

In (22) $\Delta\omega'$ indicates the dephasing rate (defined in Equation (11)) by a single TLS of energy E at a distance r from the ion, and the angular brackets now denote averaging over the TLS parameters. The function $\psi(t)$ behaves differently over different time scales, which are determined by the dephasing time. In the following sections we study two extreme time limits analytically.

4.2. Short-time behavior

Within a time shorter than the shortest spin-lattice relaxation time τ, the function

$\psi(t)$ in (22) reduces to

$$\psi(t) = 3t \int_0^\infty r^2 \langle \Delta\omega' \rangle \, \mathrm{d}r, \tag{23}$$

yielding, in view of (11),

$$\psi(t) = 3t \int \mathrm{d}E \, \rho(E) \int_0^\infty \mathrm{d}r \, r^2 V(r)^2 \operatorname{sech}^2 \left(\frac{\beta E}{2} \right) \left\langle \frac{\tau}{4\hbar^2 + \tau^2 V(r)^2} \right\rangle_E . \tag{24}$$

The subscript E of the angular brackets means that the average is for TLS with energy E. In (24), $\rho(E)$ is the normalized density of states of TLS and $V(r) = V^z$. This approximation is suitable for the situation where the dephasing rate is larger than the spin-lattice relaxation rate appropriate to high density (n) systems and to a very low temperature regime. The latter arises from the fact that the spin relaxation rate decreases faster (i.e. as $\propto T^3$) than the dephasing rate. The actual domain of validity of this approximation for a given system depends on its maximum spin-lattice relaxation rate, which is not well known in general.

For ion—TLS interaction we consider the multipolar form [16]:

$$V(r) = \frac{b}{r^s} . \tag{25}$$

Inserting (25) in (24), we obtain

$$\psi(t) = t a_s \left(\frac{b}{2\hbar} \right)^{3/s} \int \mathrm{d}E \, \rho(E) \operatorname{sech}^2 \left(\frac{\beta E}{2} \right) \langle \tau^{3/s - 1} \rangle_E . \tag{26}$$

where

$$a_s = \frac{3}{s} \int_0^\infty x^{3/s - 1} (1 + x^2)^{-1} \, \mathrm{d}x.$$

Using (15) and

$$\Gamma^{\pm} = \pi \left(\frac{E}{\hbar\omega_\mathrm{D}} \right)^3 D' \left[n(E) + \frac{1 \pm 1}{2} \right] \tag{27}$$

obtained from (14) and (8), we find [22]

$$\tau^{-1} = \pi\hbar^{-1} \left(\frac{E}{\hbar\omega_\mathrm{D}} \right)^3 D' \coth \left(\frac{\beta E}{2} \right) . \tag{28}$$

In (27), ω_D is the Debye frequency, $n(E)$ the Boson function, and

$$D' = \frac{3B^2}{Mc^2}\left(\frac{t'}{E}\right)^2. \tag{29}$$

Here M and c are the mass of a unit cell and the sound velocity, respectively. Inserting (28) in (26), defining $\rho(E) = \rho_0 E^\mu$ and $D = \langle D' \rangle_E$, we find

$$\psi(t) = \frac{3\Delta\omega t}{4\pi n}. \tag{30}$$

The lineshape is Lorentzian and the homogeneous linewidth is given by

$$\hbar\,\Delta\omega = \frac{16}{3}\pi^2 n a_s D\hbar\omega_D I_{s,\mu}\left(\frac{b}{2\pi D}\right)^{3/s}\rho_0(k_B T)^\mu\left(\frac{T}{\theta_D}\right)^{4-(9/s)} \tag{31a}$$

In (31a) θ_D is the Debye temperature and

$$I_{s,\mu} = \int_0^\infty \frac{x^{3+\mu-(9/s)}\,e^x\,dx}{(e^x+1)^{1+(3/s)}(e^x-1)^{1-(3/s)}}.$$

The constants a_s and $I_{s,\mu}$ are of the order of unity (e.g. $a_3 = \pi/2$, $I_{3,0} = 0.5$, $I_{4,0} = 0.684$). The quantity D in (31) is independent of E and can be evaluated by following the method given in Reference 22.

For a dipolar form of interaction (i.e. $s = 3$) (31a) reduces to

$$\hbar\,\Delta\omega = \tfrac{4}{3}\pi^2 n I_{3,\mu} b\rho_0(k_B T)^{1+\mu}. \tag{31b}$$

Note that the linewidth is independent of the mechanism of the spin-lattice relaxation and TLS parameters. The origin of this interesting result will be discussed later For $n\rho_0 = 2\times10^{20}/(\text{eV cm}^3)$, $b = 5.8\times10^{-36}$ erg cm^3 [21] and $\mu = 0$, we estimate $\Delta\omega = 100$ MHz at 1 K.

The temperature dependence of the homogeneous linewidth in (31) can be understood in the following way: From (11) and (25) it is clear that only those TLS lying within the radius

$$r_c = \left(\frac{\tau b}{2\hbar}\right)^{1/s} \tag{32}$$

from the ion make a significant contribution, which is given by $\hbar\,\Delta\omega'_b$ in (12b). The total contribution then arises equally from all TLS within r_c and equals

$$\frac{4}{3}\pi r_c^3 n\,\text{sech}^2\left(\frac{\beta E}{2}\right)\hbar\tau^{-1}. \tag{33}$$